JACS
JOURNAL OF THE AMERICAN CHEMICAL SOCIETY

Subscriber access provided by American Chemical Society

Article

Development of a Technique to Determine Bicyclomycin-Rho Binding and Stoichiometry by Isothermal Titration Calorimetry and Mass Spectrometry

Andrew P. Brogan, William R. Widger, Dalila Bensadek,
Isabel Riba-Garcia, Simon J. Gaskell, and Harold Kohn

J. Am. Chem. Soc., **2005**, 127 (8), 2741-2751• DOI: 10.1021/ja046441q • Publication Date (Web): 03 February 2005

Downloaded from http://pubs.acs.org on March 24, 2009

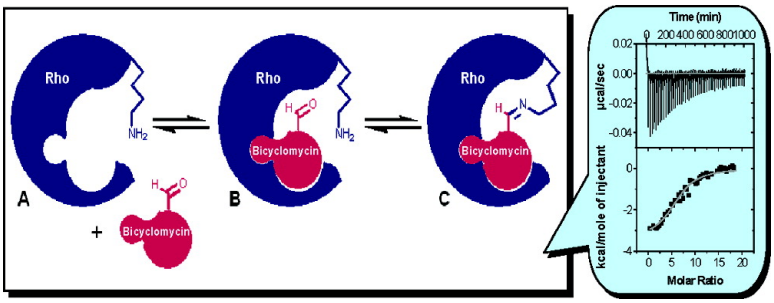

More About This Article

Additional resources and features associated with this article are available within the HTML version:

- Supporting Information
- Links to the 4 articles that cite this article, as of the time of this article download
- Access to high resolution figures
- Links to articles and content related to this article
- Copyright permission to reproduce figures and/or text from this article

View the Full Text HTML

ACS Publications
High quality. High impact.

Journal of the American Chemical Society is published by the American Chemical Society. 1155 Sixteenth Street N.W., Washington, DC 20036

J|A|C|S
ARTICLES
Published on Web 02/03/2005

Development of a Technique to Determine Bicyclomycin-Rho Binding and Stoichiometry by Isothermal Titration Calorimetry and Mass Spectrometry

Andrew P. Brogan,[†] William R. Widger,*[,‡] Dalila Bensadek,[§] Isabel Riba-Garcia,[§] Simon J. Gaskell,*[,§] and Harold Kohn*[,†]

Division of Medicinal Chemistry and Natural Products, School of Pharmacy, University of North Carolina, Chapel Hill, North Carolina 27599-7360, Department of Biology and Biochemistry, University of Houston, Houston, Texas 77204-5001, and Michael Barber Centre for Mass Spectrometry, UMIST, P.O. Box 88, Manchester M60 1QD, United Kingdom

Received June 16, 2004; Revised Manuscript Received December 15, 2004; E-mail: harold_kohn@unc.edu; widger@uh.edu; simon.gaskell@umist.ac.uk

Abstract: Bicyclomycin (**1**) is the only natural product inhibitor of the transcription termination factor rho. Rho is a hexameric helicase that terminates nascent RNA transcripts utilizing ATP hydrolysis and is an essential protein for many bacteria. The paucity of information concerning the **1**−rho interaction stems from the weak binding affinity of **1**. We report a novel technique using imine formation with rho to enhance the affinity of a bicyclomycin analogue and determine the binding stoichiometry by isothermal titration calorimetry (ITC) and mass spectrometry (MS). Our designed bicyclomycin ligand, 5a-(3-formyl-phenylsulfanyl)-dihydrobicyclomycin (**2**) (apparent $I_{50} = 4\ \mu$M), inhibits rho an order of magnitude more efficiently than **1** ($I_{50} = 60\ \mu$M). MS shows that **2** selectively forms an imine with K181 in rho. We found that despite the heterogeneity of ATP binding (three tight and three weak) imposed on the rho hexamer, the nearby bicyclomycin binding pocket is not affected, and both **1** and **2** bind with equal affinity to all six subunits.

Introduction

Cell viability requires the orderly expression of genes. In *Escherichia coli*, RNA transcripts are terminated either by a spontaneous process or by the intervention of the transcription termination factor rho.[1] It has been estimated that rho actively terminates transcription in approximately half of the open reading frames in *E. coli*.[2] Rho is a homohexameric protein arranged in a toroid shape.[3−9] Rho translocates along the mRNA and mediates the release of transcripts by disrupting RNA polymerase polynucleotide biosynthesis.[10]

Several ligand sites in rho are essential for protein function. These include two distinct RNA binding sites, termed primary and secondary, and an ATP binding site.[10] The primary, tight RNA binding sites are located in the N-terminus and span all six subunits.[11] It is the initial site for RNA binding and recognizes rut (rho utilizing) sites on the nascent transcript, characterized by high cytosine content. The primary RNA binding sites will also bind single-stranded DNA sequences with high cytosine content. The secondary RNA binding sites line the central hole and consist of basic residues (Lys, Arg) positioned at the N- and the C-terminal direction from the ATP binding site on the individual rho monomers.[12−14] Binding at the secondary sites are RNA specific, unlike the primary sites. Sequential binding of the nascent transcript at the secondary sites of the individual monomers allows rho to translocate along the mRNA.[10] RNA binds to the secondary sites less tightly than it does to the primary sites.[15,16]

Secondary site RNA binding stimulates ATP hydrolysis that, in turn, fuels rho translocation. The ATP binding site is located in the C-terminal domain at the interface of adjacent subunits. The nucleotide-binding pocket is distinguished by Walker-A and Walker-B sequence motifs with the signature P-loop at residues 175−183 in *E. coli* rho. The stoichiometry of ATP binding to rho has been investigated. Two models, a three tight-site model[17−19] and a six-site model where three of the six sites

[†] University of North Carolina.
[‡] University of Houston.
[§] Michael Barber Centre for Mass Spectrometry, UMIST.

(1) Yager, T. D.; von Hippel, P. H. In *The Molecular and Cell Biology of E. coli. and S. typhimurium*; Neidhardt, F., Ed.; The American Society of Microbiology: Washington, DC, 1987; pp 1241−1275.
(2) Zsu, A. Q.; von Hippel, P. H. *Biochemistry* **1998**, *37*, 11202−11214.
(3) Oda, T.; Takanami, M. *J. Mol. Biol.* **1972**, *71*, 799−802.
(4) Shigesada, K.; Tsurushita, N.; Imai, M. *Ann. Rep. Inst. Virus Res., Kyoto Univ.* **1978**, *21*, 72−73.
(5) Bear, D. G.; Hicks, P. S.; Escudero, K. W.; Andrews, C. L.; McSwiggen, J. A.; von Hippel, P. H. *J. Mol. Biol.* **1988**, *199*, 623−635.
(6) Gogol, E. P.; Seifried, S. E.; von Hippel, P. H. *J. Mol. Biol.* **1991**, *221*, 1127−1138.
(7) Geiselmann, J.; Yager, T. D.; Gill, S. C.; Calmettes, P.; von Hippel, P. H. *Biochemistry* **1992**, *31*, 111−121.
(8) Yu, X.; Horiguchi, T.; Shigesada, K.; Egelman, E. H. *J. Mol. Biol.* **2000**, *299*, 1279−1287.
(9) Skordalakes, E.; Berger, J. M. *Cell* **2003**, *114*, 135−146.
(10) Richardson, J. P. *Biochim. Biophys. Acta* **2002**, *1577*, 251−260.
(11) Richardson, J. P. *J. Biol. Chem.* **1982**, *257*, 5760−5766.
(12) Wei, R. R.; Richardson, J. P. *J. Biol. Chem.* **2001**, *276*, 28380−28387.
(13) Wei, R. R.; Richardson, J. P. *J. Mol. Biol.* **2001**, *314*, 1007−1015.
(14) Xu, Y.; Kohn, H.; Widger, W. R. *J. Biol. Chem.* **2002**, *277*, 30023−30030.
(15) Geiselmann, J.; Yager, T. D.; von Hippel, P. H. *Protein Sci.* **1992**, *1*, 861−873.
(16) Wang, Y.; von Hippel, P. H. *J. Biol. Chem.* **1993**, *268*, 13947−13955.

bind ATP tightly,[20−25] have been proposed. Recently, we reported the stoichiometry of adenine nucleotides with rho using a sensitive fluorescence-quenching method that allowed detection of both the tight and the weak binding sites.[25] Using the rho mutant F355W, we showed that ATP binds to three sites tightly ($K_{d1} = 3 \pm 0.3$ μM) and three sites loosely ($K_{d2} = 58 \pm 3$ μM), while ADP, the product of ATP hydrolysis, binds loosely ($K_d = 92$ μM) to essentially all six sites. The heterogeneity in ATP binding sites was observed in the absence and in the presence of single-stranded RNA (poly(C)) and DNA (poly (dC)).

Bicyclomycin (**1**), a commercial antibiotic, is the only known selective inhibitor of rho.[26] Mechanistic studies have shown that **1** is a mixed inhibitor of secondary site RNA binding[27] and is a reversible, noncompetitive inhibitor of ATP hydrolysis.[28] Bicyclomycin binding occurs at a unique site in the C-terminus of the rho protomer; this site is situated near the ATP binding site and overlaps with a portion of the secondary RNA binding sites. Rho mutational studies[29,30] and bicyclomycin affinity labels[24,31−33] suggest that **1** binds in a cleft between the α7 and the α8 helices (nomenclature based on the Skordalakes and Berger X-ray crystal structure of rho[9]), with the C(1) triol group in **1** pointed toward the outside of the rho hexamer and the terminal C(5)−C(5a) exomethylene group pointed toward the terminal γ-phosphate of ATP and the P-loop on rho.[34] Significantly, bicyclomycin inactivation of one to two subunits in rho is sufficient to halt rho ATP hydrolysis.[24] In vitro kinetic assays measuring ATP hydrolysis (not to be confused with transcription termination assays[35]) provide a K_i of 21 μM for **1,** indicating that the antibiotic binds to rho with low affinity.[28] This affinity has contributed to limited information concerning the stoichiometry of the **1**−rho hexamer complex. It is not known whether **1** binds to all six rho subunits and if there is binding heterogeneity similar to ATP.

Herein, we report the synthesis and evaluation of 5a-(3-formyl-phenylsulfanyl)-dihydrobicyclomycin (**2**), a bicyclomycin analogue designed to efficiently inhibit rho. We show that the attachment of an aryl aldehyde moiety to **1** enhances binding to rho through imine formation with a lysine residue located at the drug-binding site, increasing **2** binding affinity. We document, using mass spectrometry (MS) and isothermal titration calorimetry (ITC), that **2** binds to all six subunits, that the binding affinity of **2** is the same at all subunits, and that binding is not appreciably affected by the absence or presence of adenine nucleotides. Furthermore, reversible covalent bond formation to enhance the binding of low affinity ligands has not been previously reported, and we examine the broader implications of this novel methodology.

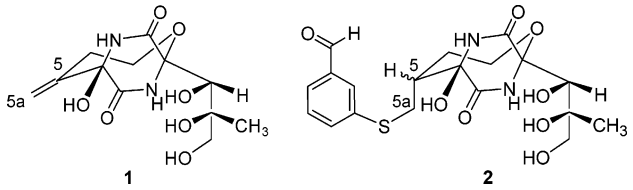

Results

1. Design Considerations for ITC and Choice of Bicyclomycin Aldehyde. The thermodynamic binding constants and stoichiometry for ligand−protein complexes can be measured by ITC.[36−40] An integral parameter in ITC measurements is the Wiseman c value[41−43] (eq 1), where $[M]_t$ is the receptor protein concentration, n is the number of binding sites per receptor, and K_d is the dissociation constant. Accurate binding isotherms and the corresponding binding stoichiometry can be determined if curve fitting is in the experimental window of $10 \leq c \leq 500$.[41−43]

$$c = \frac{n[M]_t}{K_d} \quad (1)$$

According to eq 1, low-affinity ligands require higher protein concentrations to fit within the experimental window. The K_d for the **1**−rho complex is not known, but estimates derived from K_i (21 μM) and I_{50} (60 μM) in the rho poly(C)-dependent ATPase assay indicate it is >10 μM. Thus, to obtain $c \geq 10$ and measure **1** binding to rho by ITC, the rho monomer concentration ($n[M]_t$) needs to exceed 100 μM. This corresponds to protein levels ≥5 mg/mL. Attempts to maintain an aqueous rho solution at 5 mg/mL (100 μM, based on monomer) for the duration of an ITC experiment (≈5 h, 26 °C) were unsuccessful (data not shown). However, we were able to achieve stable, aqueous rho solutions at 24 μM monomer (4 μM hexamer, 1.1 mg/mL) using relatively high KCl concentrations (400 mM) and the addition of the cofactors, poly(dC) or poly(C).

In a recent study, Turnbull and Daranas reported that binding isotherms using ITC can be determined for low-affinity systems when $c < 10$, if four criteria are met: (1) a sufficient portion of the binding isotherm is used for analysis, (2) the binding stoichiometry is known, (3) the concentrations of ligand and receptor are known with accuracy, and (4) adequate signal-to-noise is observed during the titration.[44] We measured the binding isotherm for **1** with the 24 μM rho (based on monomer) solution

(17) Stitt, B. L. *J. Biol. Chem.* **1988**, *263*, 11130−11137.
(18) Stitt, B. L.; Xu, Y. M. *J. Biol. Chem.* **1998**, *273*, 26477−26486.
(19) Stitt, B. L. *Biochemistry* **2001**, *40*, 2276−2281.
(20) Geiselmann, J.; von Hippel, P. H. *Protein Sci.* **1992**, *1*, 850−860.
(21) Kim, D. E.; Shigesada, K.; Patel, S. S. *J. Biol. Chem.* **1999**, *274*, 11623−11628.
(22) Kim, D. E.; Patel, S. S. *Biochemistry* **2000**, *39*, 1551−1552.
(23) Kim, D. E.; Patel, S. S. *J. Biol. Chem.* **2001**, *276*, 13902−13910.
(24) Vincent, F.; Widger, W. R.; Openshaw, M.; Gaskell, S. J.; Kohn, H. *Biochemistry* **2000**, *39*, 9067−9076.
(25) Xu, Y.; Johnson, J.; Kohn, H.; Widger, W. R. *J. Biol.Chem.* **2003**, *278*, 13719−13727.
(26) Zwiefka, A.; Kohn, H.; Widger, W. R. *Biochemistry* **1993**, *32*, 3564−3570.
(27) Magyar, A.; Zhang, Y. D.; Kohn, H.; Widger, W. R. *J. Biol. Chem.* **1996**, *271*, 25369−25374.
(28) Park, H. G.; Zhang, X. D.; Moon, H. S.; Zwiefka, A.; Cox, K.; Gaskell, S. J.; Widger, W. R.; Kohn, H. *Arch. Biochem. Biophys.* **1995**, *323*, 447−454.
(29) Magyar, A.; Zhang, X. D.; Abdi, F.; Kohn, H.; Widger, W. R. *J. Biol. Chem.* **1999**, *274*, 7316−7324.
(30) Moyse, K. A.; Knight, J. S.; Richardson, J. P. *J. Mol. Biol.* **2000**, *302*, 565−579.
(31) Cho, H. J.; Park, H. G.; Zhang, X. D.; Riba, I.; Gaskell, S. J.; Widger, W. R.; Kohn, H. *J. Org. Chem.* **1997**, *62*, 5432−5440.
(32) Riba, I.; Gaskell, S. J.; Cho, H. J.; Widger, W. R.; Kohn, H. *J. Biol. Chem.* **1998**, *273*, 34033−34041.
(33) Vincent, F.; Openshaw, M.; Trautwein, M.; Gaskell, S. J.; Kohn, H.; Widger, W. R. *Biochemistry* **2000**, *39*, 9077−9083.
(34) Vincent, F.; Srinivasan, J.; Santillan, A.; Widger, W. R.; Kohn, H. *J. Org. Chem.* **2001**, *66*, 2251−2264.
(35) Wu, A. M.; Christie, G. E.; Platt, T. *Proc. Natl. Acad. Sci. U.S.A.* **1981**, *78*, 2913−2917.
(36) Jelesarov, I.; Bosshard, H. R. *J. Mol. Recognit.* **1999**, *12*, 3−18.
(37) Ladbury, J. E.; Chowdhry, B. Z. *Chem. Biol.* **1996**, *3*, 791−801.
(38) Leavitt, S.; Freire, E. *Curr. Opin. Struct. Biol.* **2001**, *11*, 560−566.
(39) Ward, W. H.; Holdgate, G. A. *Prog. Med. Chem.* **2001**, *38*, 309−376.
(40) Holdgate, G. A. *BioTechniques* **2001**, *31*, 164−166, 168, 170.
(41) Wiseman, T.; Williston, S.; Brandts, J. F.; Lin, L. N. *Anal. Biochem.* **1989**, *179*, 131−137.
(42) Fisher, H. F.; Singh, N. *Methods Enzymol.* **1995**, *259*, 194−221.
(43) Indyk, L.; Fisher, H. F. *Methods Enzymol.* **1998**, *295*, 350−364.

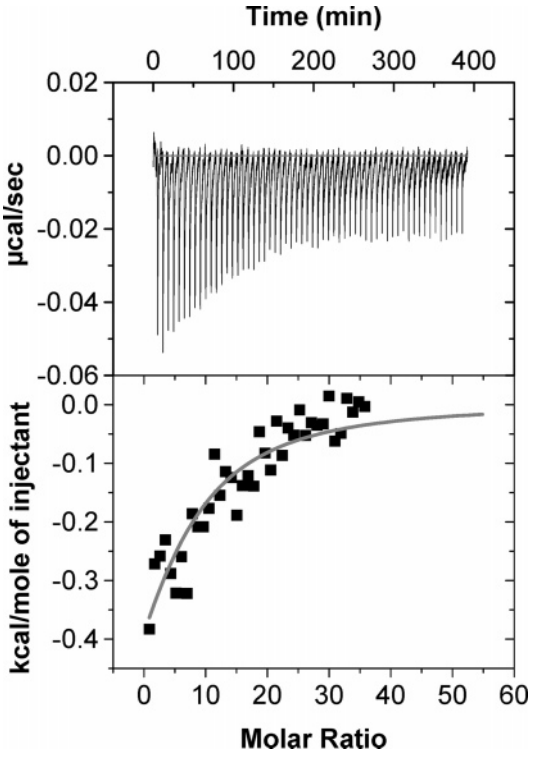

Figure 1. Example binding isotherm for the titration of **1** into a rho solution (24 μM, based on monomer; 4 mM, based on hexamer) containing poly(dC) (1.33 μM) and ATP (200 μM). (A) Raw calorimetric trace. Each peak corresponds to the thermal power evolved from the addition of 5.0 μL of **1** (1 mM) into a 1.4 mL rho solution. (B) Hyperbolic plot of normalized titration isotherm. The solid line represents the best fitting curve calculated from assuming six equal binding sites for **1** within the rho hexamer.

containing poly(dC) (1.3 μM) and ATP (200 μM) using ITC. Complete saturation of all rho primary RNA binding sites occurs with 1.3 μM poly(dC) since three to four rho hexamers (4 μM) will bind to one poly(dC) molecule given an average poly(dC) length of $\approx$450 nt. As expected, we obtained a hyperbolic binding isotherm (rather than sigmoidal), indicative of $c < 10$, that could only be analyzed assuming the stoichiometry of the **1**−rho complex (Figure 1). Assuming a stoichiometry of six, where all six sites were identical, yielded a K_d of 40.7 $\pm$ 5.0 μM and a corresponding c value of 0.6 using the Origin 5.0 fitting program (Table 1). It is noteworthy that fitting of the **1** binding isotherms to a two-type binding site model (two sets of three equal binding sites per hexamer) and assuming a maximum of six total binding sites led to two K_d values ($\approx$40 μM) that were approximately equal to each other. Attempts to fit the data to the other two binding site models with various stoichiometries using the Origin 5.0 software (e.g., five tight, one weak) led to poor fits that did not converge well. This provided the preliminary information that **1** bound to each of the subunits within the rho hexamer with equal binding affinity. Nonetheless, we needed to enhance bicyclomycin-rho binding (lower K_d) to provide c values that would allow independent determinations of the K_d and stoichiometry of the bicyclomycin−rho complex.

We previously reported that bicyclomycin aldehydes **3** and **4** reacted with lysine residues near the bicyclomycin binding site to give the bound imine (Figure 2, A $\rightleftharpoons$ C) and that imine formation was reversible.[24,31] We further demonstrated that $NaBH_4$ treatment of the bicyclomycin bound imine gave the irreversibly modified amine (Figure 2, C $\rightarrow$ D). ESI-MS was used to analyze the reductive amination rho products obtained from **3** and **4**. We found that **3** (1 mM) bound $\approx$45% of the available monomers,[31] and MS/MS analysis of trypsin-treated **3**-bound rho showed that the lysine residue K181 was selectively modified.[32] Correspondingly, **4** (400 μM) modified approximately five of the six subunits,[24] and adduction occurred at K336.[33] In the present study, we examined whether we could exploit the ease with which bicyclomycin aldehydes undergo reversible imine formation to promote bicyclomycin binding to rho. We anticipated that imine adduction would improve the binding affinity of the bicyclomycin derivative.

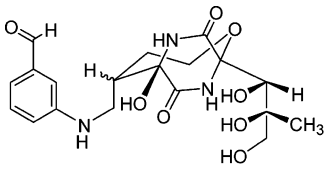

3

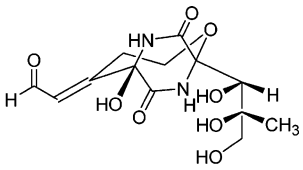

4

We required a bicyclomycin aldehyde that efficiently bound all six subunits with high affinity. Neither **3** or **4** was satisfactory. Bicyclomycin aldehyde **3** (1 mM) modified only half of the subunits after $NaBH_4$ reduction.[31] Furthermore, the apparent I_{50} for **3** in the poly(C)-dependent ATPase assay was 70 μM, placing this compound on par with **1** (60 μM).[31] Correspondingly, **4** (400 μM) modified five of the six sites after $NaBH_4$ treatment.[24] However, when the inhibition of **4** was measured in the poly(C)-dependent ATPase assay, we obtained an apparent I_{50} of 35 μM and a K_i of 62 μM.[24] These findings indicated that the binding affinities of **3** and **4** did not substantially differ from **1**, making both compounds unsuitable for ITC stoichiometric measurements.

Bicyclomycin aldehyde **3** is a substituted dihydrobicyclomycin where an aniline substituent is tethered to the 5a site. We previously documented that 5a-thio-substituted dihydrobicyclomycins exhibited excellent rho inhibitory activities and that their activities typically exceeded their nitrogen counterparts.[45,46] For example, the I_{50} for 5a-(phenylsulfanyl)-dihydrobicyclomycin (**5**) was 75 μM while 5a-(anilino)-dihydrobicyclomycin (**6**) was 120 μM. These findings led us to choose **2**, the sulfur analogue of **3**, for synthesis and evaluation.

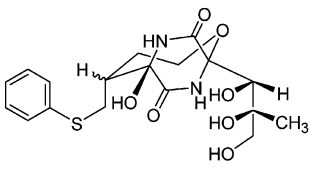

5

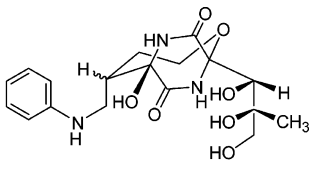

6

2. Synthesis and Characterization of 5a-(Phenylsulfanyl)-dihydrobicyclomycin (2). Synthesis of **2** proceeded in four steps (Scheme 1). Treatment of 1 with 2,2-dimethoxypropane and *p*-toluenesulfonic acid gave 2′,3′-acetonide **7**.[47] Dissolution of

(44) Turnbull, W. B.; Daranas, A. H. *J. Am. Chem. Soc.* **2003**, *125*, 14859−14866.

(45) Park, H.; Zhang, Z. M.; Zhang, X. D.; Widger, W. R.; Kohn, H. *J. Org. Chem.* **1996**, *61*, 7764−7776.

(46) Brogan, A. P.; Widger, W. R.; Kohn, H. *J. Org. Chem.* **2003**, *68*, 5575−5587.

(47) Kamiya, T.; Maeno, S.; Kataura, Y. Belgium Patent (847−475), 1976.

Table 1. Isothermal Titration Calorimetry. Titration of Hexameric Rho (4 μM Rho, Based on Hexamer) with **1** or **2** at 26 °C

ligand (titrant)	poly-nucleotide	adenosine nucloteide	K_d (μM)	ΔG_b (kcal/ mol)	ΔH_b (kcal/mol)	$T\Delta S_b$ (kcal/mol)	n^a	c^b
1	poly(dC)	ATP	40.7 ± 5.0	-6.01 ± 0.08	-0.79 ± 0.72	5.22 ± 0.80	6[c]	0.6
2	poly(dC)	ATP	2.5 ± 1.8	-7.70 ± 0.44	-2.74 ± 0.94	4.95 ± 0.24	6.1 ± 2.2	10
2	poly(dC)	none	6.3 ± 0.2	-7.12 ± 0.02	-1.34 ± 0.62	5.78 ± 0.26	6[c]	4

[a] n = stoichiometry of binding, based on hexameric rho. [b] Wiseman c value.[41−43] [c] Stoichiometry of six was fixed for this value prior to fitting.[44] All values reported are the average of two independent experiments ± two times the standard deviation.

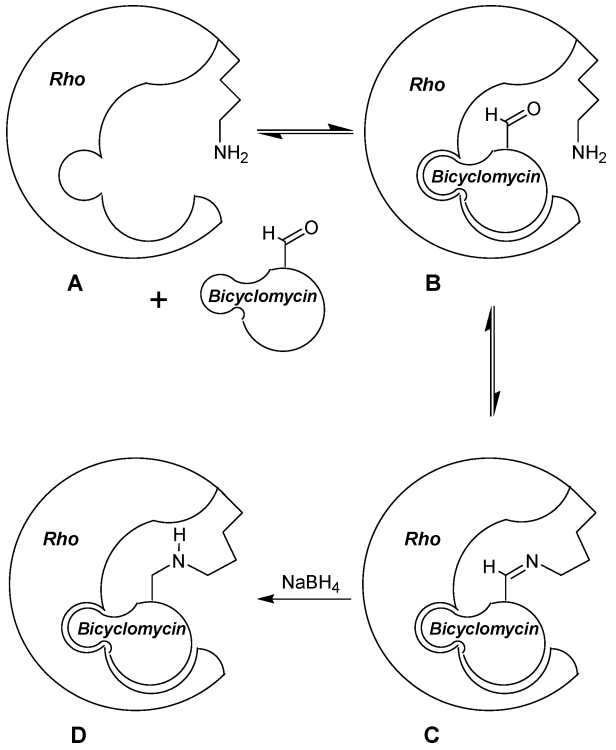

Figure 2. Proposed mode of action of bicyclomycin reductive amination probes **2**−**4**.

Scheme 1. Preparation of 5a-(3-Formyl-phenylsulfanyl)-dihydrobicyclomycin (**2**)

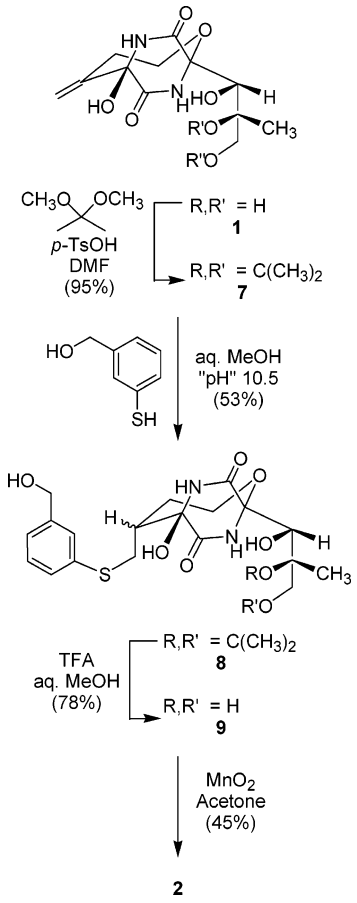

7 with 3-mercaptobenzyl alcohol[48] in 50% aqueous methanol adjusted to pH 10.5 yielded the Michael addition adduct **8** as a mixture of diastereomers (≈3:1, NMR analysis). Deprotection of the acetonide group in **8**, using TFA, gave **9**. Careful oxidation of the benzyl alcohol unit with MnO_2 provided aldehyde **2** without competitive oxidation of the sulfide linkage, in 18% overall yield (four steps).

The spectroscopic data (IR, ^{1}H NMR, ^{13}C NMR, low- and high-resolution mass spectrometry) for **2** were in agreement with its proposed structural assignment. Diagnostic NMR signals for **2** were the appearance of the aldehyde proton at δ 9.94 in the ^{1}H NMR[49] and the detection of the aldehyde carbon at 193.8 ppm in the ^{13}C NMR.[50] Aldehyde **2** was isolated as a diastereomeric mixture. We were unable to separate the isomers by PTLC. For **6,** X-ray crystallographic analysis showed that the major isomer corresponded to the C(5)-*S* isomer.[45] Bicyclomycin aldehyde **2** was routinely stored as a solid (−80 °C) for months without apparent decomposition (TLC and NMR analysis).

3. Biochemical and Biological Studies. The rho poly(C)-dependent ATPase assay[51] serves as a reliable test of rho inhibition, and any compound that was ineffective in this assay displayed little or no antimicrobial activity against W3350 *E. coli*.[34,45,46,52] Accordingly, we tested **2** in this assay and found it to be the most efficient inhibitor of rho in vitro activity to date. It had an apparent I_{50} of 4 μM, an order of magnitude lower than the parent compound **1** (I_{50} = 60 μM) and the previous bicyclomycin reductive amination probes **3** (apparent I_{50} = 70 μM) and **4** (apparent I_{50} = 35 μM). The improved inhibitory activity of **2** as compared with **3** was consistent with expectation.[45,46] The factors, however, that contributed to this improved bioactivity remain unclear. Recently, we obtained an X-ray crystallographic structure for **2** bound to rho.[53] The aryl unit in **2** extended out of the bicyclomycin binding pocket and nestled between the hydrophobic side chain of P180 of one monomer and the aliphatic portion of the side chain of K336 from the adjacent monomer. The terminal aldehyde of this

(48) Thurber, T. C.; Prince, A.; Halpern, O. *J. Heterocycl. Chem.* **1982**, *19*, 961−965.
(49) Jackman, L. M.; Sternhell, S. *Applications of Nuclear Magnetic Resonance Spectroscopy in Organic Chemistry*; Permagon Press: Oxford, 1969.
(50) Stothers, J. B. *Carbon-13 NMR Spectroscopy*; Academic Press: New York, 1972.
(51) Sharp, J. A.; Galloway, J. L.; Platt, T. *J. Biol. Chem.* **1983**, *258*, 3482−3486.
(52) Santillan, A.; Zhang, X. D.; Widger, R.; Kohn, H. *J. Org. Chem.* **1998**, *63*, 1290−1298.
(53) Skordalakes, E.; Brogan, A. P.; Park, B. S.; Kohn, H.; Berger, J. M. *Structure*, **2005**, *13*, 99−109.

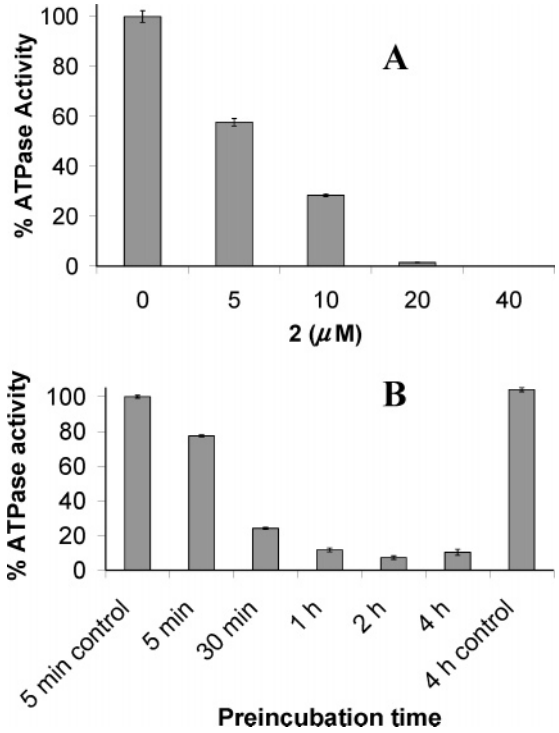

Figure 3. (A) Histogram depicting percent of rho ATPase activity after preincubation (2−4 h) with **2** followed by reductive amination with $NaBH_4$ (60 mM, final concentration) and centrifugation through a Bio-spin 6 column at various concentrations of **2**. (B) Histogram depicting the required preincubation time for maximum imine formation. Addition of $NaBH_4$ (60 mM, final concentration) at various preincubation times at a fixed **2** concentration (10 μM). Control is without **2**.

moiety appeared to be able to hydrogen bond to K181, but the poor electron density for this section of the molecule suggested that the thiobenzaldehyde unit is mobile. The C(5) stereochemistry in **2** could not be assigned because of the resolution (2.90 Å) of the X-ray crystallographic structure. Since we do not have a comparable image for **3** with rho, we do not know if the same binding interactions seen in the **2**−rho structure exist for **3**. Little antimicrobial activity was observed for **2** when measured against W3350 *E. coli* in a filter disk assay.[54] The minimum inhibitory concentration (MIC) for **2** was only 16 mg/mL, while the MIC for **1** in a control experiment was 0.21 mg/mL. The lack of antimicrobial activity for **2** was in agreement with previous findings for this class of 5a-substituted dihydrobicyclomycins.[45]

Next, we determined whether **2** served as a reductive amination probe. Incubation of rho (1 μM, based on monomer) and poly(C) (40 nM) with various concentrations of **2** (0−40 μM) followed by treatment with $NaBH_4$ led to permanent loss of rho ATPase activity (Figure 3A). Increasing loss of ATPase activity was observed with increasing **2** concentrations and 100% loss of activity at 40 μM. The addition of **1** (5 mM) prohibited the irreversible inactivation of rho ATPase activity by **2**, indicating that **1** and **2** bind to the same site in the protein (data not shown). We also examined the incubation time required for maximum reductive amination by **2**. When solutions containing rho (1 μM, based on monomer), poly(C) (40 nM), and a fixed concentration of **2** (10 μM) were preincubated for various times (0−4 h) followed by $NaBH_4$ reduction, we observed a time to maximum imine formation of 2 h (Figure 3B) if we assume that $NaBH_4$ reduction of the **2**−rho imine is rapid. These

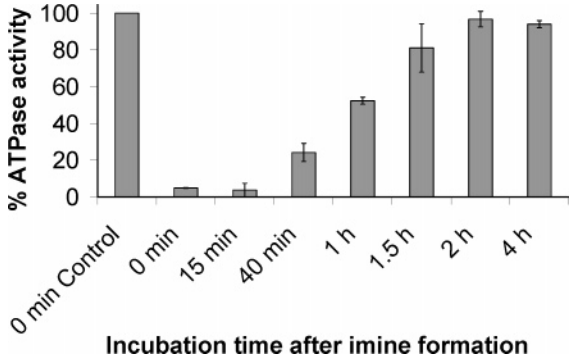

Figure 4. Histogram depicting the reversibility of **2**−rho imine formation by measuring percent of rho ATPase activity at various time points after passage through a Bio-Spin 6 column using a fixed concentration of **2** (10 μM). Control is without **2**.

findings indicate that **2** is a more efficient reductive amination probe with rho than its predecessors **3**[31] and **4**,[24] with 100% loss of ATPase activity at **2** concentrations of $\geq$40 μM and maximum imine formation occurring at 2 h when rho concentrations are 1 μM (based on monomer).

Analysis of **3** and **4** in previous studies[24,31] indicated that the imines formed with rho are transient and that full recovery of rho ATPase activity occurs upon dissolution in buffer solutions at 1 h for **3**[31] and at 24 h for **4**.[24] These findings indicate that the **3**−rho imine was less stable than the **4**−rho imine. We recognized that the reversibility of the **2**−rho complex as an important parameter to consider when designing our ITC experiments. Accordingly, we determined the reversibility of the **2**−rho transformation by measuring the incubation time required for recovery of rho poly(C)-dependent ATPase activity. Solutions containing rho (1 μM, based on monomer), poly(C) (40 nM), and a fixed concentration of **2** (10 μM) were incubated for 2 h, and unbound **2** was removed by passage through a Biospin-6 column. The rho ATPase activity was measured after various incubation times following removal of unbound **2** (0−4 h) (Figure 4). We found that after spin column treatment, **2** forms a moderately stable rho−imine and that the **2**−rho interaction is a reversible process with full recovery of ATPase activity after 2 h. Thus, the apparent I_{50} for **2** likely corresponds to a combination of structural complementarity with the bicyclomycin binding pocket in rho and **2**−rho imine formation.

We proceeded to determine the K_i for **2** using the kinetics of the rho poly(C)-dependent ATPase assay. The Lineweaver−Burk plot of $1/V$ versus [ATP] at various **2** concentrations shown in Figure 5A was obtained using the Enzyme Kinetics Module 1.1 for SigmaPlot 2001 and revealed noncompetitive inhibition ($R^2 = 0.984$) with a $K_i = 6$ μM. Similar to the I_{50} values observed for **1**−**4**, the K_i for **2** is significantly lower than that of **1** ($K_i = 21$ μM), **3** ($K_i = 27$ μM), and **4** ($K_i = 62$ μM). To ensure that **2**−rho imine formation inhibited rho ATPase activity by a reversible noncompetitive pathway with respect to ATP, we measured the velocity of ATP hydrolysis (V_{max}) as a function of total rho concentration (125−1000 nM, based on monomer) in the presence of **2** (5 μM). We compared these results with **1** (60 μM) and reactions performed in the absence of inhibitor. Plots of V_{max} versus [rho] without inhibitor (control), **1** (60 μM), and **2** (5 μM) yielded straight lines that all intersected

(54) Ericsson, H. M.; Sherris, J. C. *Acta Pathol. Microbiol. Scand. B: Microbiol. Immunol.* **1971**, *217*, Suppl.

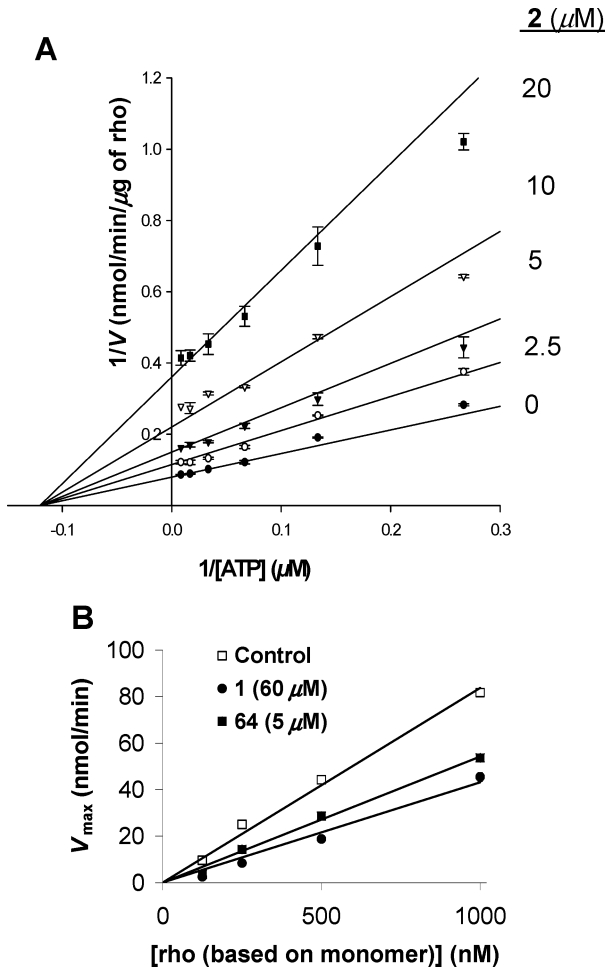

Figure 5. (A) Lineweaver−Burk plot of the poly(C)-dependent ATPase activity of rho at varying **2** concentrations obtained from the Enzyme Kinetics Module 1.1 in SigmaPlot 2001. (B) Plot of V_{max} vs [rho]. All lines intersect the origin indicating reversible inhibition.

the origin, indicating reversible noncompetitive inhibition (Figure 5B).[55]

Collectively, our findings from the inhibition profile, imine formation, and reductive amination of **2** are consistent with previous bicyclomycins where **1**, **3**, and **4** were found to be reversible, noncompetitive inhibitors of rho ATP hydrolysis.

4. Mass Spectrometry. Previous examination of **3** and **4** reductive amination with rho by ESI−MS indicated that **3** modified ≈45% of the rho monomers,[31] while **4** modified five out of six rho monomers.[24] Comparative analysis of the ESI−MS maximum entropy processed spectra showed a peak that corresponds to a mass of 47 002 Da for native rho and a mass of 47 428 Da for the irreversible **2**−rho adduct (Figure 6). This 426 Da mass shift for **2**-modified rho correlates well with the expected monoisotopic shift of *m*/*z* 425.1322. The ESI−MS results indicate modification of five and two-tenths out of the six rho subunits that comprise the hexamer using 100 μM **2**.

The modification site within the rho protomer was identified by analyzing the tryptic digests of both unmodified and **2**-modified rho. Comparative analyses of the tryptic digests by MALDI−MS revealed the presence of a singly charged ion at *m*/*z* 1474.99 in the **2**−rho adduct sample, which was absent in the spectrum of native rho (MALDI data not shown). When ESI−MS analysis was performed, the ions at *m*/*z* 737.80 and 492.23 were observed in the modified **2**−rho spectra and corresponded to the doubly and triply protonated species from the singly charged ion at *m*/*z* 1474.99 observed by MALDI. If the ion at *m*/*z* 1474.99 (MH^+) is a modified fragment, then the mass of the unmodified fragment must be 1473.99−424.13 = 1049.86 Da. This mass is unique to the tryptic fragment T23−24 (residues 174−184; GLIVAPPKAGK), making it a good candidate for modification by **2** since it contains an internal lysine residue.

With this hypothesis in mind, the site of **2** modification was further investigated by tandem MS experiments. The product ion spectra were recorded for the doubly and the triply charged precursor ions, *m*/*z* 737.80 and 492.23, respectively. The fragment ions generated in the collision induced dissociation (CID) experiments allowed the identification of the following N-terminal partial sequence tag (G,L)IVAX$_n$ (Figure 7). Since this sequence occurs only once in the complete rho sequence, it allowed the unequivocal identification of the modified tryptic peptide as T23−24. This modified fragment contains two lysine residues (K181 and K184). However, since a modified lysine would not be recognized by trypsin as a cleavage site, K181 is identified as the site of modification. Furthermore, the y_1 ion corresponding to the unmodified K184 residue was observed in both tandem MS analyses. The higher *y*-series fragment ions (y_4−y_8) have a mass shift of 424 Da, consistent with K181 modification by reductive amination with **2**. Other *y*-series ions (y_5−y_8) with a mass increment of 314 Da were also observed, suggesting additional fragmentation of the adducted moiety. Together, these results allowed us to identify K181 as the site of modification, in keeping with previous studies with **3**.[32]

5. Isothermal Titration Calorimetry (ITC). We have shown the time to maximum imine formation of a solution containing 10 μM **2** and 1 μM rho (based on monomer) was 2 h (Figure 3B). The formation of the reversible **2**−rho imine is likely a second-order process that depends on the concentrations of both **2** and rho. We took this into consideration when designing our ITC experiments and recognized that by using 24 μM rho (based on monomer), the reaction parameters for imine formation would be altered from those previously measured (Figures 3 and 4). Accordingly, we varied the time between injections (400−1200 s) and found that a 1200 s interval between injections of **2** was sufficient for the heat evolved to return to the baseline value from this reversible binding/imine formation process (a priori). An adequate return to the baseline value was not observed with shorter time intervals (data not shown). By comparison, the time between injections with **1** was 400 s. We obtained a sigmoidal binding isotherm, indicative of $c \geq 10$, by titrating **2** (400 μM, 5 μL injections) into a solution of rho (24 μM, based on monomer) containing poly(dC) (1.3 μM) and ATP (200 μM) (Figure 8). Using the Origin 5.0 software and the rho hexamer concentration, the binding isotherm for **2** converged and fit best to a single type of binding site model with a K_d of 2.5 ± 1.8 μM, a binding stoichiometry of 6.1 ± 2.2, and a corresponding *c* value of 10 (Table 1). Similar to the ITC data obtained from **1**, fitting of the **2** binding isotherms to a two-type binding site model led to two K_d values ≈3 μM.

We further examined the **2**−rho interaction by changing the conditions of the rho solution by omitting the nucleotide (Table

(55) Segel, I. H. *Enzyme Kinetics*; John Wiley & Sons: New York, 1975; pp 127−128.

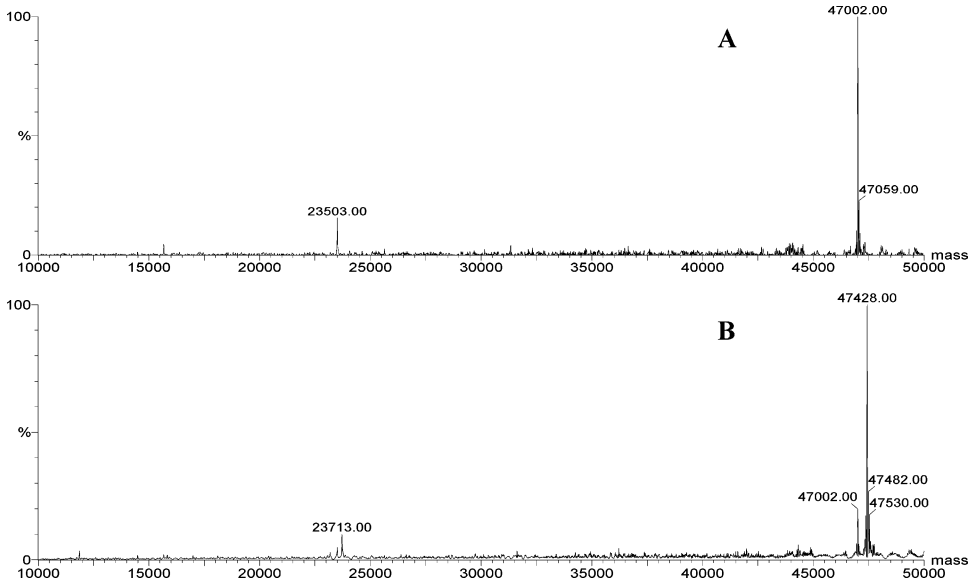

Figure 6. Maximum entropy processed spectrum obtained from ESI-QTOF-MS of (A) unmodified rho protein (1.5 μM) and (B) modified rho (1.5 μM) subjected to reductive amination using **2** (100 μM). The mass shift of 426 Da corresponds to **2**-modified rho.

1). We observed modest increases in K_d (decreased affinity) for **2** binding when rho solutions (24 μM, based on monomer) containing poly(dC) (1.3 μM) and no nucleotide ($K_d = 6.3 \pm 0.2$ μM) were compared with the initial ATP (200 μM) ($K_d = 2.5 \pm 1.8$ μM) conditions. We assumed a six equal binding site model for these binding isotherms since $c < 10$ from the increase in K_d.

A unique attribute of ITC is the ability to measure the thermodynamic binding parameters ΔG_b, ΔH_b, and ΔS_b. In our case, we can compare the thermodynamics of ligand **1**, which binds to the protein noncovalently, with a similar ligand **2**, which binds and also forms a reversible imine bond with the protein. When examining the binding thermodynamics from the ITC measurements of **1** and **2** under the same conditions (Table 1, poly(dC) and ATP), we find a difference in $\Delta\Delta G_b \approx 1.7$ kcal/mol that corresponds to a similar difference in $\Delta\Delta H_b$ ($\approx$2.0 kcal/mol) and only a small change in $T\Delta S_b$ ($\Delta T\Delta S_b \approx$ 0.3 kcal/mol). Furthermore, the ΔH_b for **1** is only -0.79 kcal/mol, indicating that **1** binding is driven by the entropy term. A larger ΔH_b was observed for **2** ($\Delta H_b = -2.74$ kcal/mol), suggesting that the difference in binding from **1** and **2** is driven by the enthalpy term that likely corresponds to the thermodynamics of imine bond formation of **2** with K181 in rho. Further examination of the thermodynamic parameters of **2** binding in the absence of adenine nucleotide revealed only modest changes in ΔG_b. These results indicate that, in the presence of poly(dC), bicyclomycin binding is not appreciably affected by either the absence or the presence of nucleotide.

Discussion

Bicyclomycin is the only natural product inhibitor of the transcription termination factor rho. The weak binding of **1** has led to limited information on the **1**−rho interaction. We report the design, synthesis, and evaluation of 5a-(3-formyl-phenylsulfanyl)-dihydrobicyclomycin (**2**), the most efficient inhibitor of the rho in vitro activity to date. Examination of the **2**−rho interaction by MS and ITC indicated that **2** binds equally to all six rho hexamer subunits in the presence and absence of ATP. Further extrapolation of the ITC data allowed us to assign **1** binding equally to all six subunits since in our ITC studies with **2** we concluded that there are a total of six bicyclomycin binding sites within the rho hexamer and that all subunits bind **2** with the same affinity. In a recent X-ray crystallographic study, we provided structural data for **1**, **2**, and **4** bound to rho.[53] This study further validates the equality of the bicyclomycin binding sites within the rho hexamer. Current crystallization conditions only permit rho to be crystallized in the lock washer conformation. This conformation is an inactive ATPase with a 10−12 Å gap between two of the rho monomers. Electron density for **1**, **2**, and **4** was observed in five of the six subunits. The inhibitor was absent from the protomer that did not have a completely formed binding pocket as a result of the gap in the hexameric ring. Crystallization of the closed ring form of the rho hexamer is ongoing; nonetheless ITC, MS, and X-ray crystallographic studies all point toward bicyclomycin binding equally to all six subunits within the rho hexamer. This is an intriguing discovery considering the heterogeneity of binding observed for the nearby ATP binding pocket. Previously, we reported a bicyclomycin fluorescent probe (BFP) that allowed us to measure BFP and ATP binding to the three tight ATP binding sites using fluorescence resonance energy transfer (FRET).[46] FRET measurements are distance dependent, and we were also able to sense a conformational change in rho induced by ATP binding. This conformational change is implicated in rho tracking along the RNA transcript. Average movements $\approx$20 Å in the C-terminus were observed upon ATP binding. Apparently, the nearby α7 and α8 helices involved in **1** binding[53] are minimally affected by this nucleotide-induced movement or the heterogeneity of ATP binding within the rho hexamer. We were unable to examine the heterogeneity of BFP and ATP binding in our FRET studies since we did could not measure binding at the weak ATP binding subunits. This unanswered question was examined in the present study, and we were able to assign the binding of **1** and **2** equally to all six subunits.

In addition to defining the binding and stoichiometry of the **1**−rho interaction, we outline a novel technique that may have broader implications. ITC is a powerful tool to determine K_d

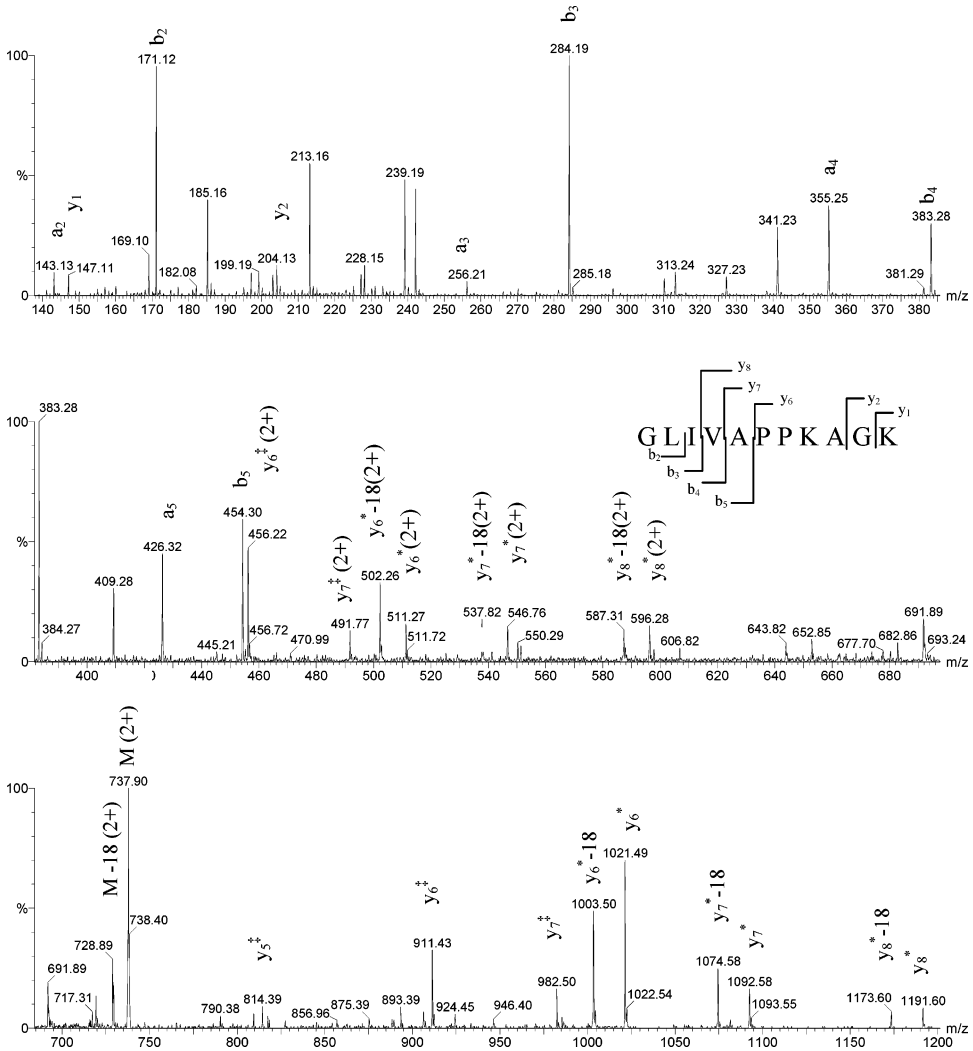

Figure 7. Product ion spectrum derived from the doubly charged ion at *m*/*z* 737.89 for the tryptic fragment T23−24 (174−184, GLIVAPPKAGK) incorporating modified K181. The *y* fragment ions labeled with * have a 424 Da mass increment in comparison with masses expected for the unmodified sequence; *y* ions labeled with ++ have a 314 Da mass increment. Note that for clarity, the spectrum is presented as three overlapping segments, with separate normalization of each segment.

and stoichiometry and is the only technique that provides direct measurement of the thermodynamics of binding. A limitation of ITC is the high protein concentrations required to stay within the experimental window $10 \leq c \leq 500$. The formation of a reversible covalent bond enhanced the affinity of our ligand and increased our c value from 0.6 to 10, permitting accurate measurements of the binding stoichiometry for **2**. There are no previous reports of ITC measurements of reversible covalent bond formation. Further analysis using the technique for low affinity ligands outlined by Turnbull and Daranas[44] enabled us to assign **1** binding equally to all six subunits of the protein.

Imine bond formation is ideally suited for the use in this reversible, covalent modification process to enhance ligand binding necessary for ITC stoichiometric measurements, but other transient bonds such as disulfide exchange, hemiacetals, and hemithioacetals could also be used. These studies allowed us to define the parameters for a broader use of this technique. First, the covalent modification of the ligand to the receptor should not perturb the binding process since distortion of this interaction may affect the ligand binding affinities. This criterion requires that the functional groups on the ligand and the receptor site be properly aligned to permit covalent adduction without alteration of the binding site. Thus, we predict that the site of covalent modification should be at a locus not involved in receptor binding and that the appended site should not affect binding of the ligand. Adherence to this criterion increases the likelihood that the ligand analogue and the ligand bind to the receptor in the same fashion. Second, the dynamics for reversible ligand covalent modification must be complete within the time interval between ITC injections allowing the system to reach equilibrium after each incremental addition of ligand. Third, the covalent modification site should not affect the binding of other ligands or cofactors necessary for receptor function, which can influence the binding of the ligand under study. In our case, **2** meets these criteria. In particular, we tethered the 3-formylphenylsulfanyl component to the 5a-position of bicyclomycin. The aryl aldehyde projects away from the cleft between the α7 and α8 helices toward the site of ATP hydrolysis.[53] Structure−activity relationship studies have shown that a wide range of substituents can be attached at this site without loss of inhibitory activity.[34,45,52] Aiding in our choice of **2** was the site of covalent amino acid attachment. Compound **2** reacts with the ϵ-amino group of K181. The four methylene units that separate the terminal amine from the peptide backbone α-carbon in K181 provide

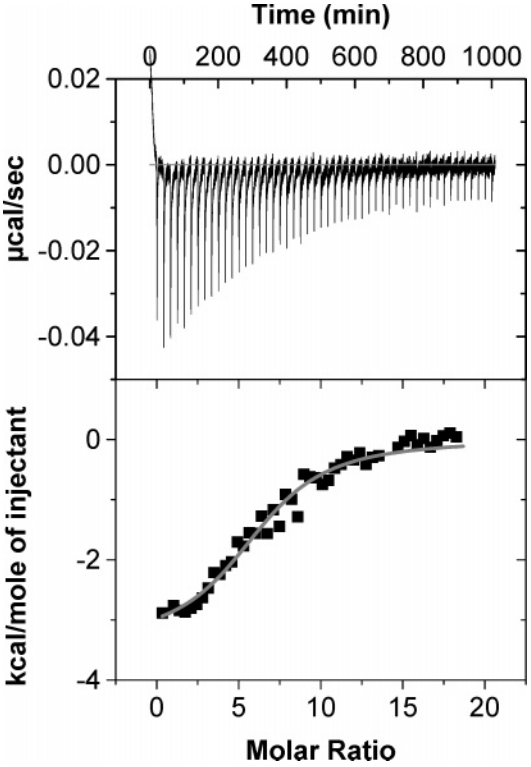

Figure 8. Example binding isotherm for the titration of **2** into a rho solution (24 μM, based on monomer; 4 μM, based on hexamer) containing poly(dC) (1.33 μM) and ATP (200 μM). (A) Raw calorimetric trace. Each peak corresponds to the thermal power evolved from the addition of 5.0 μL of **2** (400 μM) into 1.4 mL of rho solution. (B) Sigmoidal plot of normalized titration isotherm. The solid line represents the best fitting curve calculated from one type of binding site model (all sites are equal within the rho hexamer).

conformational flexibility and help ensure that the bicyclomycin−rho complex is not distorted upon imine formation.

Experimental Procedures

General Methods. Low- and high-resolution (CI) mass spectral studies were run at the University of Texas at Austin by Dr. M. Moini. Thin-layer chromatographies were run on precoated silica gel slides (20 × 20 cm; Sigma Z12272-6). Bicyclomycin was purified by three successive silica gel chromatographies using 20% MeOH-$CHCl_3$ as the eluant prior to use in biological experiments. Rho protein was isolated from *E. coli* AR 120 containing the overexpressing plasmid p39-ASE,[56] which has the wild-type E155 residue seen in the original p39-AS plasmid.[57] Rho purity was assessed by SDS−PAGE, and protein concentration was measured according to the bicinchoninic acid (BCA) method.[58] [γ-^{32}P]ATP was purchased from Perkin-Elmer (Boston, MA), and nucleotides were obtained from Sigma. Polyethyleneimine (PEI) thin-layer chromatography (TLC) plates used for ATPase assays were purchased from J. T. Baker, Inc. (Phillipsburg, NJ).

5a-(3-Hydroxymethyl-phenylsulfanyl)-dihydrobicyclomycin 2′,3′-Acetonide (8). To a methanolic solution (10 mL) of 7[47] (105 mg, 0.32 mmol) under Ar was added 3-mercaptobenzyl alcohol (300 mg, 2.14 mmol), and then the pH was adjusted to 10.5 with aqueous 1.0 M NaOH. The mixture was stirred at room temperature (8 h) until no starting material remained (TLC analysis). The pH of the mixture was adjusted to 7.0 with aqueous 0.1−1.0 M HCl. The solvent was removed in vacuo, and the residue was purified by preparative TLC (10% MeOH−$CHCl_3$) to afford **8** as a mixture of diastereomers (≈3:1): yield, 80 mg (53%); R_f 0.44 (10% MeOH−$CHCl_3$); FT-IR (KBr) 3304 (br), 2934 (br), 1690, 1395, 1045 cm^{-1}; ^{1}H NMR (CD_3OD) for the major diastereomer, δ 1.36 (s, 3 H, C(2′)CH_3), 1.45 (s, 6 H, C(CH_3)$_2$), 1.88−2.30 (m, 3 H, C(4)*H*H′, C(4)H*H*′, C(5)H), 2.53 (dd, J = 11.6, 13.9 Hz, 1 H, C(5a)*H*H′), 3.65−3.88 (m, 3 H, C(3)*H*H′, C(3′)*H*H′, C(5a)H*H*′), 3.94−4.07 (m, 1 H, C(3)H*H*′), 4.09 (s, 1 H, C(1′)H), 4.45 (d, J = 8.7 Hz, 1 H, C(3′)H*H*′), 4.56 (s, 2 H, C(3″)CH_2OH), 7.13−7.19 (m, 1 H, Ar), 7.24−7.31 (m, 2 H, Ar), 7.34 (s, 1 H, C(2″)H); ^{1}H NMR (CD_3OD) for the minor diastereomer, δ 1.44 (s, 6 H, C(CH_3)$_2$), 2.77 (dd, J = 11.6, 13.9 Hz, 1 H, C(5a)*H*H′), 4.46 (d, J = 8.7 Hz, 1 H, C(3′)H*H*′), 4.57 (s, 2 H, C(2″)CH_2OH), the remaining peaks overlapped with nearby signals and were not resolved; the structural assignments were in agreement with the ^{1}H−^{1}H COSY experiment; ^{13}C NMR (CD_3OD) for the major diastereomer, 24.9, 26.9, 28.3, 30.4, 33.4, 51.9, 63.5, 64.9, 73.2, 73.4, 83.7, 86.3, 88.7, 111.7, 125.6, 128.2, 128.5, 130.1, 137.4, 143.8, 168.0, 171.6 ppm; ^{13}C NMR (CD_3OD) for the minor diastereomer, 25.0, 28.4, 31.7, 63.7, 83.7, 86.4, 89.0, 111.7, 125.7, 128.7, 130.1, 143.9 ppm, the remaining peaks overlapped with nearby signals and were not resolved; MS (+CI) 483 [M + 1]$^+$; M_r (+CI) 483.181 01 [M + 1]$^+$ (calcd for $C_{22}H_{31}N_2O_8S$ 483.180 11).

5a-(3-Hydroxymethyl-phenylsulfanyl)-dihydrobicyclomycin (9). To a 50% aqueous methanolic solution (10 mL) containing **8** was added TFA (eight drops), and then the solution was stirred at room temperature (20 h) until no starting material remained (TLC analysis). The solvent was removed in vacuo, and the residue was purified by preparative TLC (20% MeOH−$CHCl_3$) to afford **9** (65 mg, 0.13 mmol) as a mixture of diastereomers (≈3:1): yield, 45 mg (78%); R_f 0.32 (20% MeOH−$CHCl_3$); FT-IR (KBr) 3300 (br), 2908 (br), 1688, 1405, 1042 cm^{-1}; ^{1}H NMR (CD_3OD) for the major diastereomer, δ 1.33 (s, 3 H, C(2′)-CH_3), 1.93−2.30 (m, 3 H, C(4)*H*H′, C(4)H*H*′, C(5)H), 2.58 (dd, J = 11.6, 13.9 Hz, 1 H, C(5a)*H*H′), 3.52 (d, J = 11.3 Hz, 1 H, C(3′)*H*H′), 3.61−4.06 (m, 4 H, C(3)*H*H′, C(3)H*H*′, C(5a)H*H*′, C(3′)H*H*′), 4.04 (s, 1 H, C(1′)H), 4.56 (s, 2 H, C(3″)CH_2OH), 7.12−7.17 (m, 1 H, Ar), 7.23−7.29 (m, 2 H, Ar), 7.37 (s, 1 H, C(2″)H); ^{1}H NMR (CD_3OD) for the minor diastereomer, δ 1.34 (s, 3 H, C(2′)CH_3), 2.75 (dd, J = 11.6, 13.9 Hz, 1 H, C(5a)*H*H′), 3.55 (d, J = 11.3 Hz, 1 H, C(3′)*H*H′), 4.06 (s, 1 H, C(1′)H), 4.57 (s, 2 H, C(3″)CH_2OH), the remaining peaks overlapped with nearby signals and were not resolved; the structural assignments were in agreement with the ^{1}H−^{1}H COSY experiment; ^{13}C NMR (CD_3OD) for the major diastereomer, 24.2, 30.1, 33.0, 51.8, 62.2, 64.9, 68.5, 72.2, 78.2, 83.7, 89.4, 125.6, 128.2, 128.6, 130.1, 137.4, 143.7, 168.6, 172.1 ppm; ^{13}C NMR (CD_3OD) for the minor diastereomer, 30.4, 32.0, 63.2, 72.3, 78.2, 83.6, 89.6, 125.6, 128.1, 130.1, 137.5, 143.8, 167.6, 174.0 ppm, the remaining peaks overlapped with nearby signals and were not resolved; MS (+CI) 443 [M + 1]$^+$; M_r (+CI) 443.147 17 [M + 1]$^+$ (calcd for $C_{19}H_{27}N_2O_8S$ 443.148 81).

5a-(3-Formyl-phenylsulfanyl)-dihydrobicyclomycin (2). To an acetone solution containing **9** (9 mg, 0.02 mmol) was added MnO_2 (50 mg, 0.58 mmol) in five portions (10 mg each) over 7 h. The mixture was stirred at room temperature until no starting material remained (TLC analysis). The mixture was filtered and concentrated in vacuo. The residue was redissolved in MeOH and isolated by preparative TLC (20% MeOH−$CHCl_3$) to afford **2** as a mixture of diastereomers (≈3:1): yield, 4 mg (45%); R_f 0.42 (20% MeOH−$CHCl_3$); FT-IR (KBr) 3266 (br), 2935 (br), 1691, 1403, 1043 cm^{-1}; ^{1}H NMR (CD_3OD) for the major diastereomer, δ 1.33 (s, 3 H, C(2′)CH_3), 1.91−2.32 (m, 3 H, C(4)*H*H′, C(4)H*H*′, C(5)H), 2.65 (dd, J = 11.6, 13.9 Hz, 1 H, C(5a)*H*H′), 3.53 (d, J = 11.3 Hz, 1 H, C(3′)*H*H′), 3.63−4.07 (m, 4 H, C(3)*H*H′, C(3)H*H*′, C(5a)H*H*′, C(3′)H*H*′), 4.03 (s, 1 H, C(1′)H), 7.45−7.55 (m, 1 H, Ar), 7.65−7.73 (m, 2 H, Ar), 7.88−7.93 (m, 1 H, C(2″)H), 9.94 (s, 1 H, C(3″)C(H)O); ^{1}H NMR (CD_3OD) for the minor diastereomer, δ 2.82 (dd, J = 11.6, 13.9 Hz, 1 H, C(5a)*H*H′), 3.55 (d, J = 11.3 Hz, 1 H, C(3′)*H*H′), 4.07 (s, 1 H, C(1′)H), 9.95 (s, 1 H, C(3″)C(H)O), the remaining peaks overlapped with nearby signals and

(56) Nehrke, K. W.; Seifried, S. E.; Platt, T. *Nucleic Acids Res.* **1992**, *20*, 6107.
(57) Mott, J. E.; Grant, R. A.; Ho, Y. S.; Platt, T. *Proc. Natl. Acad. Sci. U.S.A.* **1985**, *82*, 88−92.
(58) Smith, P. K.; Krohn, R. I.; Hermanson, G. T.; Mallia, A. K.; Gartner, F. H.; Provenzano, M. D.; Fujimoto, E. K.; Goeke, N. M.; Olson, B. J.; Klenk, D. C. *Anal. Biochem.* **1985**, *150*, 76−85.

were not resolved; the structural assignments were in agreement with the $^1H-^1H$ COSY experiment; ^{13}C NMR (CD_3OD) for the major diastereomer, 24.2, 30.1, 32.8, 51.8, 62.1, 68.5, 72.3, 78.2, 83.7, 89.4, 127.7, 130.2, 130.8, 135.0, 138.7, 139.6, 168.7, 172.0, 193.8 ppm; ^{13}C NMR (CD_3OD) for the minor diastereomer, 30.6, 31.9, 53.5, 63.2, 83.6, 89.7, 127.8, 130.0, 130.9, 139.7 ppm, the remaining peaks overlapped with nearby signals and were not resolved; MS (+CI) 441 $[M + 1]^+$; M_r (+CI) 441.134 59 $[M + 1]^+$ (calcd for $C_{19}H_{25}N_2O_8S$ 441.133 16).

General Procedure 1. Inhibition of Rho Poly(C)-Dependent ATPase Activity.[51] The ribonucleotide-stimulated ATPase activity of rho at 32 °C was assayed by the amount of ^{32}P-labeled inorganic phosphate hydrolyzed from ATP after separation on PEI-TLC plates (prerun with water and dried) using 0.75 M potassium phosphate (pH 3.5) as the mobile phase. Reactions (100 μL) were initiated by ATP (250 μM) and 0.5 μCi [γ-^{32}P]ATP being added to solutions containing inhibitor (0−400 μM), poly(C) (300 nM), and rho (300 nM, based on monomer) in buffer (40 mM Tris HCl (pH 7.9), 50 mM KCl, and 12 mM $MgCl_2$). Solutions were preincubated for 2 h at 25 °C and 90 s at 32 °C prior to the addition of ATP. Five aliquots (0.7 μL) were removed at 15 s intervals during the assay and spotted onto PEI-TLC plates. The TLC plates were exposed to PhosphorImager plates (Fuji and Molecular Dynamics) (15 h), scanned on a Storm 860 PC PhosphorImager, and analyzed using Molecular Dynamic's ImageQuant 5.0. The initial rates of the reactions were determined by plotting the amount of ATP hydrolyzed against time. Each assay was performed in duplicate, and the results were averaged.

Kinetics of Rho Poly(C)-Dependent ATPase Activity. ATPase assays were carried out as described in General Procedure 1. Reactions (100 μL) were initiated by various concentrations of ATP (3.75, 7.5, 15, 30, 60, and 120 μM) and 0.5 μCi [γ-^{32}P] ATP being added to solutions containing poly(C) (100 nM) and rho (100 nM, based on monomer) in buffer (40 mM Tris HCl (pH 7.9), 50 mM KCl, and 12 mM $MgCl_2$). Five aliquots (0.7 μL) were taken at various times (5−20 s) depending upon the ATP concentrations and spotted onto PEI-TLC plates. Each series was repeated in the presence of **2** (0−20 μM). Solutions were preincubated for 2 h at 25 °C and 90 s at 32 °C prior to the addition of ATP. The initial rates for each ATP concentration were plotted using the Enzyme Kinetics Module 1.1 for SigmaPlot 2001. Each assay was performed in duplicate, and the results were averaged.

Assay Testing Bicyclomycin (1) and 5a-(3-Formyl-phenylsulfanyl)-dihydrobicyclomycin (2) Reversibility. A modified version of General Procedure 1 was employed by the ATP hydrolysis being measured at various concentrations of rho (125−1000 nM, based on monomer) with poly(C) (500 nM) and either **1** (60 μM), **2** (5 μM), or no inhibitor in buffer (40 mM Tris HCl (pH 7.9), 50 mM KCl, and 12 mM $MgCl_2$). Reactions (100 μL) were initiated by ATP (250 μM) and 0.5 μCi [γ-^{32}P]ATP being added, and five aliquots (0.7 μL) were removed at 5−15 s intervals during the assay and spotted onto PEI-TLC plates. Plots of the initial rates versus [rho, based on monomer] were made to determine if the inhibitors were reversible. Each assay was performed in duplicate, and the results were averaged.

General Procedure 2. Reductive Amination of Rho.[24,31−33] A solution (200 μL) containing buffer (40 mM Tris HCl (pH 7.9), 50 mM KCl, and 12 mM $MgCl_2$), rho (1 μM, based on monomer), ATP (1 mM), poly(C) (40 nM), and **2** (0−100 μM) was incubated at 25 °C (2−4 h). An aqueous solution (20 μL) of $NaBH_4$ (600 mM, freshly made) was added, and the reaction was allowed to incubate at 25 °C (20 min).

Reductive Amination of Rho using Various Concentrations of 5a-(3-Formyl-phenylsulfanyl)-dihydrobicyclomycin (2). General Procedure 2 for the reductive amination of rho was employed using **2** (0−40 μM). After reductive amination, 2 μL of 10 mg/mL bovine serum albumin (BSA) (0.1 mg/mL BSA, final concentration) was added to the reaction mixture, and 100 μL aliquots were added to Biospin-6 columns (Bio-Rad, Inc.) preequilibrated with buffer (40 mM Tris HCl (pH 7.9), 50 mM KCl, and 12 mM $MgCl_2$) containing 0.1 mg/mL BSA. The Biospin-6 columns were centrifuged at 4000 rpm (4 °C) for 5 min. Aliquots (40 μL) from the centrifuged filtrates were diluted into buffer (40 mM Tris HCl (pH 7.9), 50 mM KCl, and 12 mM $MgCl_2$) containing poly(C) (300 nM) and were assayed for poly(C)-dependent ATPase activity using General Procedure 1.

Preincubation Time for Rho−Imine Formation with 5a-(3-Formyl-phenylsulfanyl)-dihydrobicyclomycin (2). Using General Procedure 2 and 10 μM **2**, solutions were allowed to preincubate for various times (5, 30, 60, 120, 240 min) before $NaBH_4$ was added. After reductive amination, 2 μL of 10 mg/mL bovine serum albumin (BSA) (0.1 mg/mL BSA, final concentration) was added to the reaction mixture, and 100 μL aliquots were added to Biospin-6 columns preequilibrated with buffer (40 mM Tris HCl (pH 7.9), 50 mM KCl, and 12 mM $MgCl_2$) containing 0.1 mg/mL BSA. The Biospin-6 columns were centrifuged at 4000 rpm (4 °C) for 5 min. Aliquots (40 μL) from the centrifuged filtrates were diluted into buffer (40 mM Tris HCl (pH 7.9), 50 mM KCl, and 12 mM $MgCl_2$, total volume: 100 μL) containing poly(C) (300 nM) and were assayed for poly(C)-dependent ATPase activity using General Procedure 1.

5a-(3-Formyl-phenylsulfanyl)-dihydrobicyclomycin (2)−Rho Imine Adduct: Stability versus Time. A solution (200 μL) containing buffer (40 mM Tris HCl (pH 7.9), 50 mM KCl, and 12 mM $MgCl_2$), rho (1 μM, based on monomer), ATP (1 mM), poly(C) (40 nM), and **2** (10 μM) was incubated at 25 °C (2 h). After incubation, 2 μL of 10 mg/mL bovine serum albumin (BSA) (0.1 mg/mL BSA, final concentration) was added to the reaction mixture, and 100 μL aliquots were added to Biospin-6 columns preequilibrated with buffer (40 mM Tris HCl (pH 7.9), 50 mM KCl, and 12 mM $MgCl_2$) containing 0.1 mg/mL BSA. The Biospin-6 columns were centrifuged at 4000 rpm (4 °C) for 5 min. Aliquots (40 μL) from the centrifuged filtrates were diluted into buffer (40 mM Tris HCl (pH 7.9), 50 mM KCl, and 12 mM $MgCl_2$, total volume: 100 μL) containing poly(C) (300 nM), allowed to incubate at various times (0, 15, 40, 60, 90, 120, 240 min), and then assayed for poly(C)-dependent ATPase activity using General Procedure 1.

Mass Spectrometry: Detection of 5a-(3-Formyl-phenylsulfanyl)-dihydrobicyclomycin (2)-Modified Rho. The reductive amination of rho (1 μM, based on monomer, 0.5−1 mL) by **2** (0−100 μM) was conducted using General Procedure 2. After reductive amination, the samples were dialyzed (4 °C, 20 h) against buffer (10 mM Tris HCl (pH 7.9), 100 mM NaCl, 5% glycerol, 0.1 mM EDTA, and 0.1 mM DTT). Aliquots (40 μL) from the dialysis were diluted into buffer (40 mM Tris HCl (pH 7.9), 50 mM KCl, and 12 mM $MgCl_2$) containing poly(C) (300 nM) and assayed for poly(C)-dependent ATPase activity using General Procedure 1. The remainder of the samples was sent to UMIST in dialysis buffer at room temperature. The samples were desalted using $ZipTip_{C18}$ pipet tips (Millipore, Billerica, MA), using sequential elution with acetonitrile/water (20:80 by volume with 0.1% formic acid) in the first instance and acetonitrile/water (80:20 by volume with 0.1% formic acid) in the second elution. The protein fractions were pooled together to give a final concentration of 1.5 μM protein in acetonitrile/water (50:50 by volume with 0.1% formic acid). A portion of the eluate was used directly for MS analysis. Electrospray MS analyses were performed using a hybrid quadrupole time-of-flight (Q-TOF) mass spectrometer (Micromass, Ltd., Manchester, UK). The capillary potential was held at 3.5 kV, and the cone was set at 45−46 V. Samples were introduced via a syringe driver (Harvard Apparatus, South Natick, MA) at a constant flow rate of 0.5 μL/min. The m/z range of 400−1600 was recorded. Spectra were accumulated for 7 min under the control of Masslynx software (Micromass) and were processed using maximum entropy.

Mass Spectrometry: Full Tryptic Digestion of the 5a-(3-Formyl-phenylsulfanyl)-dihydrobicyclomycin (2)-Modified Rho. The reductive amination of rho (3 μM, based on monomer, 0.5−1 mL) in the presence of poly(C) (120 nM) by **2** (0, 50 μM) was conducted using General Procedure 2. After reductive amination, the samples were

dialyzed (4 °C, 20 h) against buffer (10 mM Tris HCl (pH 7.9), 100 mM NaCl, 5% glycerol, 0.1 mM EDTA, and 0.1 mM DTT). Aliquots (40 μL) from the dialysis were diluted into buffer (40 mM Tris HCl (pH 7.9), 50 mM KCl, and 12 mM $MgCl_2$) containing poly(C) (300 nM) and assayed for poly(C)-dependent ATPase activity using General Procedure 1. The remainder of the samples was sent to UMIST in dialysis buffer at room temperature. A portion of the dialysate was treated with a solution of trypsin in 2 mM $CaCl_2$ to give an enzyme/substrate ratio of 1:50. The solution was incubated at 37 °C for 18 h, after which the digestion was terminated by addition of formic acid to a final concentration of 5 vol %. The peptide products of the digestion were desalted using $ZipTip_{C18}$ pipet tips (Millipore, Billerica, MA), using sequential elution with acetonitrile/water (20:80 by volume with 0.1% formic acid) followed by acetonitrile/water (80:20 by volume with 0.1% formic acid). The two eluates were pooled together, and a portion was used for MALDI-MS analysis performed on a Voyager DE-STR (Applied Biosystems, Framingham). A portion (10 μL) of the eluate was analyzed by ESI−MS and tandem MS using a Micromass Q-TOF instrument equipped with an electrospray source and nanospray source, respectively. For MS analysis, the sample was introduced using a syringe driver (Harvard Apparatus) set to deliver a flow rate of 0.5 μL/min. For tandem MS, a 3 μL portion of the desalted digest was introduced into a gold-coated borosilicate glass capillary with a 1 μm tapered tip (Micromass). To obtain the spectrum shown in Figure 7, a doubly charged ion corresponding to an *m*/*z* value of 737.80 was selected as the precursor ion and subjected to collisional activation, using a laboratory collision energy of 48−58 eV and an indicated (manifold) pressure of argon collision gas of 5×10^{-5} mbar. Fragment ions are labeled according to the nomenclature of Biemann.[59] C-terminal (*y*-type) fragment ions, which retain the modified lysine residue, are accompanied by satellite ions arising from partial loss of the moiety derived from **2**. The product ion spectrum of the triply charged precursor ion ($[M + 3H]^{3+}$) analogue ($m/z = 492.23$) was also recorded and was entirely consistent with the proposed structure.

Inhibitory Properties of Bicyclomycin (1) and 5a-(3-Formylphenylsulfanyl)-dihydrobicyclomycin (2) in the Antimicrobial Assay.[54] Aliquots (200 μL) from suspensions of overnight LB broth cultures (*E. coli* W3350) were diluted into LB broth (2 mL). The suspension was poured onto 15 mL volume LB agar plates. The solution was gently rocked to distribute the cells evenly over the surface of the plates, and any excess cell solution was removed by pipet. The plates were incubated at 37 °C (30 min), and an antibiotic−assay disk (0.25 in. diameter) containing 20 μL of the test compound (1, 2, 4, 8, 16, 32 mg/mL in 50−100% DMSO) was placed on the agar surface. The plates were incubated at 37 °C (18 h). Data plots of the zone of inhibited bacterial growth (cm^3) versus log(1000*C*), where *C* is the concentration of the test compound (mg/mL), yielded linear slopes to provide the minimal inhibitory concentrations (MIC) for bicyclomycin and bicyclomycin derivatives. Each assay was performed in duplicate, and the results were averaged.

Isothermal Titration Calorimetry. Purified rho was dialyzed two times against 500 mL of buffer (40 mM Tris HCl (pH 7.9), 400 mM KCl, 0.1 mM EDTA, and 0.1 mM DTT) at 4 °C. After dialysis, the protein concentration was determined by the BCA method. The rho solution from dialysis was diluted (24 μM, based on monomer) into the same buffer solution that contained poly(dC) (1.3 μM) or poly(C) (4 μM) and either ATP (200 μM) or without nucleotide. The concentration of the ligand in the syringe was 400 μM for **2** or 1 mM for **1** in the identical buffer from the dialysis to minimize the heats of dilution. ITC experiments were performed using the high precision VP−ITC (MicroCal, Inc.) at 26 °C. Prior to titration, all the solutions were degassed. The titration schedule consisted of 50−60 consecutive injections of 5 μL with a 400 or 1200 s interval between injections. The values for the last five injections were averaged and subtracted from each point of the experimental trace isotherm to correct for the heats of dilution and nonspecific binding of the bicyclomycin to rho. Curve fitting was undertaken in Origin 5.0 using the standard noninteracting one or two site model supplied by MicroCal using the hexamer concentration of rho (4 μM). In experiments where $c < 10$, the stoichiometry parameter was fixed to six, or for the two site model, two integers with a sum of six. The values reported in Table 1 are the average of two experiments ± two times the standard deviation.

Acknowledgment. We thank Dr. Y. Itoh and the Fujisawa Pharmaceutical Co., Ltd., Japan, for the gift of **1**, Dr. T. Platt (University of Rochester) for the overproducing strain of rho, Dr. A. Tripathy of UNC's Macromolecular Interactions Facility for assistance with the ITC experiments, and Drs. Verna Frasca and John F. Brandts (MicroCal, LLC) for review of our ITC experiments. The American Chemical Society Division of Medicinal Chemistry and Bristol-Myers Squibb are gratefully acknowledged for support of a predoctoral fellowship to A.P.B. This investigation was supported by NIH Grant GM37934 and the Robert A. Welch Foundation Grant E1381 (W.R.W.).

Supporting Information Available: Binding isotherm for the titration of **2** into a rho solution containing poly(dC). This material is available free of charge via the Internet at http://pubs.acs.org.

JA046441Q

(59) Biemann, K. *Biomed. Environ. Mass Spectrom.* **1988**, *16*, 99−111.